Hu, Peng; Cao, Zhixian

Numerical Modeling of Hyperconcentrated Turbidity Currents

NUMERICAL MODELING OF HYPERCONCENTRATED TURBIDITY CURRENTS

Peng Hu[1], Zhixian Cao[2]

[1] PhD candidate, State Key Laboratory of Water Resources and Hydropower Engineering Science, Wuhan University, Wuhan, 430072, China.

[2] Corresponding author, Professor, State Key Laboratory of Water Resources and Hydropower Engineering Science, Wuhan University, Wuhan, 430072, China. E-mail: zxcao@whu.edu.cn.

ABSTRACT

Previous investigations of turbidity currents are mostly focused on dilute currents. Present understanding of the mechanism of hyperconcentrated turbidity currents is still limited. Abrupt transitions in hyperconcentrated turbidity currents have been observed in fixed volume lock release experiments (Hallworth & Huppert, 1998: *Physics of Fluids*, 10, 1083-1087). However, a reasonable explanation of this phenomenon has so far remained missing. A fully coupled layer-averaged mathematical model is proposed for turbidity currents incorporating the non-Newtonian nature at high sediment concentrations. The model is numerically solved using the Total-Variation-Diminishing version of the second-order Weighted Average Flux method along with the SLIC approximate Riemann solver and the MINBEE limiter. Abrupt transitions in hyperconcentrated turbidity currents are reproduced by the proposed model in a qualitative sense. This allows for the proposition that the non-Newtonian nature may be responsible for the occurrence of abrupt transitions in hyperconcentrated turbidity currents. This finding appears to indicate that existing models for turbidity currents need to be modified to incorporate the non-Newtonian nature at high concentrations in order to be generally applicable.

Keywords: hyperconcentrated turbidity currents, abrupt transition, non-Newtonian fluid

1. INTRODUCTION

Turbidity currents, which occur whenever fluid of one density intrudes into an ambient fluid, are driven by the buoyancy force due to the difference between the bulk density of the intruding fluid and that of the ambient fluid (Simpson, 1997; Hallworth and Huppert, 1998; Huppert, 2006). They have been continuously studied, including field observations, laboratory experiments and mathematical modeling, as they occur in numerous man-made and natural situations and are important to the management of water quality and morphology in inland and ocean waters (Inman *et al*. 1976; Middleton, 1993; Simpson, 1997; Kneller and Buckee, 2000; Cesare *et al*. 2001; Oehy and Schleiss, 2007). Field observations are prohibitively difficult to make because of the need to work underwater and the potential destructive effects on apparatus (Inman *et al*. 1976; Parker *et al*. 1986). Therefore, experimental and numerical methods have been frequently employed to reveal insights into the mechanism of turbidity currents (Huppert and Simpson, 1980; Rottman and Simpson, 1983; Bonnecaze *et al*. 1993, 1995; Dade and Huppert, 1995). All these works have yielded excellent agreement between experimental and numerical methods. However, they are mostly focused on dilute turbidity currents. Actually, turbidity currents can often be hyperconcentrated, such as those generated by the catastrophic

slumping of unconsolidated sediment on continental slopes in submarine areas (Parker *et al*. 1986; Hallworth and Huppert, 1998). Current understanding of the characteristics and mechanism of hyperconcentrated turbidity currents are far from clear.

Abrupt transitions in hyperconcentrated turbidity currents have been observed in a systematic series of fixed volume lock release experiments by Hallworth and Huppert (1998). They find that hyperconcentrated turbidity currents propagate rapidly the same as the dilute turbidity currents at the slump stage, however, beyond a threshold initial concentration (0.275 in Hallworth and Huppert, 1998), the former exhibits a pronounced and sudden arrest, and the arrest becomes progressively closer to the release point as the initial concentration increases. Amy *et al*. (2005) ascribes the cause of abrupt transitions in hyperconcentrated turbidity currents to low Reynolds number in laboratory through new experiments on nonparticulate solute driven density currents. Since that the characteristic of the mixtures may be distinct qualitatively between water-solute mixture and water-sediment mixture, the analogy between solute driven density currents and particle driven turbidity currents may open to be question. A reasonable explanation of the abrupt transitions in hyperconcentrated turbidity currents has to date remained missing.

Considering that water-sediment mixtures at high concentration situations may behave as non-Newtonian fluid (Qian and Wan, 1983; Pierson and Scott, 1985; Major and Pierson, 1992; Gani, 2004), a fully coupled layer-averaged mathematical model for turbidity currents is proposed incorporating the non-Newtonian nature at high concentrations. The fully coupled model is numerically solved using the Total-Variation-Diminishing (TVD) version of the second-order Weighted Average Flux (WAF) method along with the (SLIC) approximate Riemann solver and the MINBEE limiter. The proposed model is employed to investigate the physical cause of abrupt transitions in hyperconcentrated turbidity currents.

2. MATHEMATICAL FORMULATIONS

2.1 Complete governing equations

Consider layer-averaged formulation of turbidity currents over an erodible bed that is composed of uniform sediment with particle diameter d, complete governing equations include the mass and momentum conservation equations for the water-sediment mixture and the mass conservation equations respectively for sediment and bed material (Hu and Cao, 2008). They are

$$\frac{\partial h}{\partial t}+\frac{\partial hu}{\partial x}=e_w u+\frac{E-D}{1-p} \tag{1}$$

$$\frac{\partial hu}{\partial t}+\frac{\partial}{\partial x}\left(hu^2+\frac{1}{2}g'h^2\right)=-g'h\frac{\partial z}{\partial x}-\frac{(\rho_w-\rho)e_w u^2}{\rho}-\frac{u(E-D)(\rho_0-\rho)}{\rho(1-p)}-\frac{\tau}{\rho}(1+r_w) \tag{2}$$

$$\frac{\partial hc}{\partial t}+\frac{\partial huc}{\partial x}=E-D \tag{3}$$

$$\frac{\partial z}{\partial t}=-\frac{E-D}{1-p} \tag{4}$$

where t = time, x = streamwise coordinate, h = turbidity current thickness, u = layer-averaged velocity, c = layer-averaged volumetric sediment concentration, z = bed elevation, τ = shear stress, r_w = ratio of upper-interface resistance to bed resistance, e_w = water entrainment coefficient, ρ_w, ρ_s = densities of water and sediment respectively, $\rho = \rho_w(1-c) + \rho_s c$ = density of the water-sediment mixture, $\rho_0 = \rho_w p + \rho_s(1-p)$ = density of the saturated bed, $g' = Rgc$ = reduced gravity, $R = (\rho_s - \rho_w)/\rho$ = submerged specific gravity of sediment, g = gravitational acceleration, E, D = sediment entrainment and deposition fluxes arising from sediment exchange with bed, p = bed sediment porosity, $-\partial z/\partial x$ = bed slope, initially equal to S_b.

The two terms on the right hand side (RHS) of Eq. 1 quantify the rate of water entrainment and the rate of bed deformation respectively. The 2nd and 3rd terms on RHS of Eq. 2 represent the momentum transfers due to water entrainment and sediment exchange with the bed respectively and the 4th term represents the resistance force including the upper-interface and bed resistance, through which the non-Newtonian nature at high concentrations can be incorporated and may influence the evolution of hyperconcentrated turbidity currents.

2.2 Empirical relationships

To close the governing equations, several empirical relationships are introduced. The water entrainment coefficient is determined as (Parker *et al*. 1986)

$$e_w = \frac{0.00153}{0.0204 + Ri} \tag{5}$$

where $Ri = u^2/Rgch$ is Richardson number. Sediment entrainment and deposition fluxes are estimated by

$$E = \omega E_s, \quad D = \omega c_b (1-c_b)^m \tag{6a, b}$$

where $m = 4.45 R_p^{-0.1}$ is the exponent denoting the effects of hindered settling, $R_p \equiv \omega d/\nu$ is particle Reynolds number, ν = kinematic viscosity of water, ω = sediment settling velocity, calculated using formula of Zhang and Xie (1993). E_S and c_b represent the entrainment coefficient and near bed concentration, which are estimated respectively as (Parker *et al*. 1986)

$$E_S = \begin{cases} 0.3 & \psi \geq 13.2 \\ 3\times 10^{-12}\psi^{10}(1-5\psi^{-1}) & 5.0 < \psi < 13.2 \\ 0 & \psi \leq 5.0 \end{cases}, \qquad c_b = [1 + 31.5(\frac{u_*}{w})^{-1.46}]c \tag{7a, b}$$

where $\psi = (\sqrt{Rgd}/\nu)^{0.6} u_* / \omega$, u_* = bed shear velocity, calculated by (Parker *et al*. 1986)

$$u_*^2 = c_D u^2 \tag{8}$$

where c_D is bed drag coefficient.

The Bingham model is tentatively employed to determine the shear stress, thus

$$\tau = \tau_0 + \tau_B \tag{9}$$

where τ_0 is bed shear stress, and τ_B the Bingham yield stress, estimated respectively by the simple functional relationships (Parker *et al*. 1986; Qian and Wan, 1983)

$$\tau_0 = \rho u_*^2, \quad \tau_B = kc^\beta \tag{10a, b}$$

where k, β are empirical parameters. When the sediment concentration is not sufficiently large, the Bingham yield stress would be negligible, thus turbidity currents would behave as Newtonian fluid. On the contrary, the non-Newtonian nature would be notable and considerably modify the evolution of hyperconcentrated turbidity currents.

3. NUMERICAL ALGORITHM

The governing equations constitute a fourth-order hyperbolic system, which should be solved using numerical algorithms that can capture shocks waves and contact discontinuities, as of Toro (2001). With a simple form, the bed deformation Eq. 4 is separated from the remaining three equations. Given this observation, Eqs. 1, 2 and 3 are rearranged as

$$\frac{\partial \mathbf{U}}{\partial t} + \frac{\partial \mathbf{F}}{\partial x} = \mathbf{S} \tag{11}$$

where

$$\mathbf{U} = \begin{bmatrix} h \\ hu \\ hc \end{bmatrix}, \quad \mathbf{F} = \begin{bmatrix} hu \\ hu^2 + g'h^2/2 \\ huc \end{bmatrix}, \tag{12a, b}$$

$$S = \begin{bmatrix} e_w + (E-D)/(1-p) \\ -g'h\dfrac{\partial z}{\partial x} - \dfrac{u(E-D)(\rho_o - \rho)}{\rho(1-p)} - \dfrac{(\rho_w - \rho)e_w u^2}{\rho} - \dfrac{\tau}{\rho}(1+r_w) \\ E - D \end{bmatrix} \tag{12c}$$

Eq. 11, written in terms of the conservative variables of Eq. 12a, is not in a perfect conservation form due to the existence of the spatial gradient of bed elevation, as given in Eq. 12c. However, if the term is viewed as source term, an explicit discretization of Eq. 11 gives

$$\mathbf{U}_i^{adv} = \mathbf{U}_i^n - \frac{\Delta t}{\Delta x}[\mathbf{F}_{i+1/2} - \mathbf{F}_{i-1/2}] \tag{13}$$

$$\mathbf{U}_i^{n+1} = \mathbf{U}_i^{adv} + \Delta t \mathbf{S}(\mathbf{U}_i^{adv}) \tag{14}$$

where Δt = time step, Δx = spatial step, i = spatial node index, n = time step index, and $\mathbf{F}_{i+1/2}$ = numerical flux at $x = x_{i+1/2}$. The scheme is monotone and has linear stability condition

$$Cr \equiv \Delta t \max(|\lambda_{1,2,3}|)/\Delta x < 1 \tag{15}$$

where $\lambda_{1,2,3}$ are the three eigenvalues of the Jacobian matrix $\partial \mathbf{F} / \partial \mathbf{U}$.

Bed deformation is computed from Eq. 4 using the state information due to Eq. 14,

$$z_i^{n+1} = z_i^n + \Delta t \frac{(D-E)_i^{n+1}}{1-p} \tag{16}$$

The numerical fluxes in Eq. 13 are computed following a 2nd-order TVD scheme that is extension of the 1st-order centred FORCE scheme. The SLIC solver, which is of the slope-limiter type, non-upwind and results from replacing the Godunov flux by the FORCE flux in the MUSCL-Hancock scheme, is employed in this study and the details can be found in Toro (2001).

4. ABRUPT TRANSITIONS IN HYPERCONCENTRATED TURBIDITY CURRENTS

The present study aims to demonstrate that the non-Newtonian nature at high concentration situations may be responsible for the occurrence of the abrupt transitions in hyperconcentrated turbidity currents. This is substantiated by comparing the numerical results of the turbidity currents generated in laboratory by Hallworth and Huppert (1998) in two cases, i.e., incorporating and neglecting the non-Newtonian nature at high concentrations respectively.

4.1 Experiments by Hallworth and Huppert (1998)

A systematic series of experiments on turbidity currents are conducted by Hallworth and Huppert (1998), in which abrupt transitions are observed for hyperconcentrated turbidity currents. Figure 1 is the schematics of the experimental setup. The channel is horizontal and measures 2 m long, 0.2 m wide and 0.25 m deep. The location of lock gate x_0 = 0.03 m. Initial water-sediment mixture and ambient water depth h_0 = 0.10 m. The initial concentration c_0 ranges from 0.025 to 0.40, d = 0.009 mm, g = 9.8 m/s^2, ν = 1E-6 m^2/s, ρ_w = 1000 kg/m^3, and ρ_s = 3217 kg/m^3.

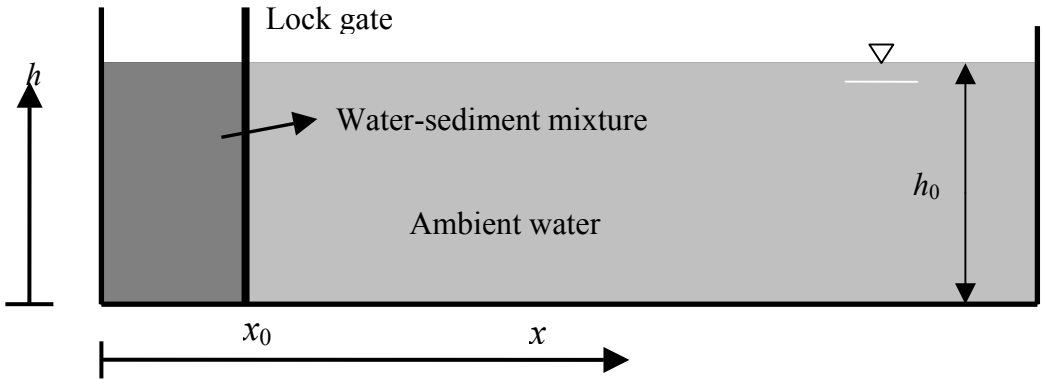

Figure 1. Schematics of the experimental setup (Hallworth and Huppert, 1998)

Abrupt transitions in hyperconcentrated turbidity currents can be most effectively illustrated by the advance the current front and the deposition geometry. Figure 2 gives the

experimental results by Hallworth and Huppert (1998) with permission of AIP, (a) the position of the current front versus t; and (b) the deposit density versus x. The deposit density is the local deposition mass D normalized by the total deposition mass M_0. From Figure 2 it is observed that hyperconcentrated turbidity currents propagate rapidly the same as dilute turbidity currents during the slump stage in the vicinity of release, however, beyond a threshold concentration (0.275 in Figure 2), the former experienced a pronounced and sudden arrest (Figure 2), depositing their sediment close to the release point, featuring step geometry (Figure 2b). The arrest becomes progressively closer to the release point and the deposition becomes steeper as the initial sediment concentration increases (Figure 2). A reasonable and qualitative explanation of this phenomenon has still remained missing to date.

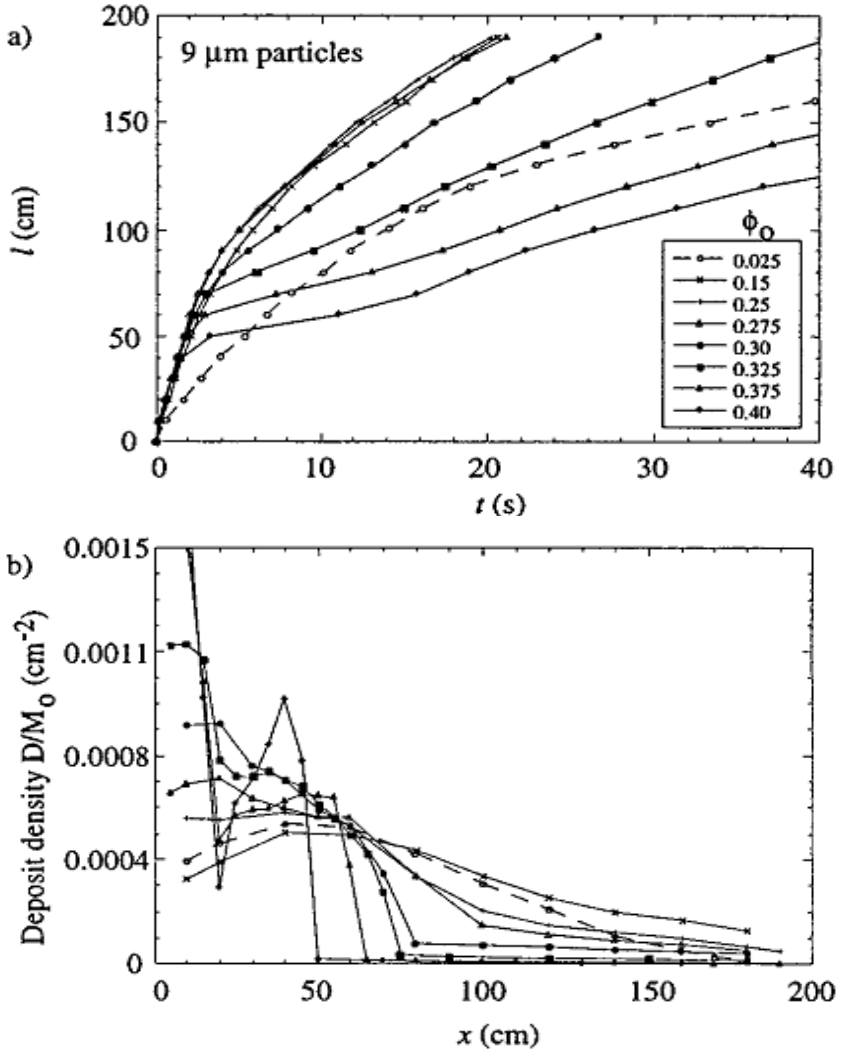

Figure 2. Experimental results by Hallworth and Huppert (1998), with permission of AIP. (a) position of the current front versus t; and (b) deposit density versus x, using various initial sediment concentrations

4.2 Comparison of numerical simulations

The occurrence of abrupt transitions in hyperconcentrated turbidity currents is addressed by comparing the numerical results in two cases. Case 1 treats turbidity currents as Newtonian fluid by specifying $k = 0.0$ N/m^2 and $\beta = 0.0$, while Case 2 considers the Non-Newtonian nature at high concentrations by prescribing $k = 10000.0$ N/m^2 and $\beta = 8.0$ (see Eq. 10b). Other parameters are consistent between Case 1 and Case 2, some of which have been presented in the prior section, and the remaining are $p = 0.4$, $c_D = 0.02$, $r_w = 0.43$. The upstream boundary conditions are specified by mass conservation of the water-sediment mixture and sediment. Numerical modeling is performed within a time period before the current front reaches the downstream boundary, therefore the boundary conditions can be set at the initial static status.

Figure 3 presents the computed position of the current front versus t using six different initial concentrations for Case 1, and Figure 4 for Case 2. In Figure 3 for Case 1, when turbidity currents are treated as Newtonian fluid, turbidity currents with larger c_0 propagate invariably faster than that with relatively lower c_0. This is because the driving force results from the density difference between the turbidity currents and the ambient water. The larger the initial concentration, the greater the driving force, thus the faster current propagates. This is in accordance with the general knowledge of turbidity currents (Huppert and Simpson, 1980; Rottman and Simpson, 1983; Bonnecaze *et al*. 1993, 1995; Dade and Huppert, 1995), but in contradiction with the abrupt transitions in hyperconcentrated turbidity currents (Hallworth and Huppert, 1998). Except for the driving force, there must be some other factors, which can greatly influence the evolution of hyperconcentrated turbidity currents. In Figure 4 for Case 2, when the non-Newtonian nature at high concentrations is incorporated in the modeling, the propagation of turbidity currents are subdued to a certain extent (in comparison with Figure 3 for Case 1), and abrupt transitions appear ($c_0 > 0.25$ in Figure 4). This is because turbidity currents have to overcome the Bingham yield stress arising from the non-Newtonian nature. Specifically, when the initial concentration is not sufficiently large ($c_0 \le 0.25$ in Figure 4), the Bingham yield stress is relatively small and the effects of non-Newtonian nature are inconsiderable in comparison with the driving force. Therefore the relationship between the initial concentration and the advance of current front is similar to that in Case 1. However, as the initial concentration increases and exceeds a threshold value (say, 0.25 in Figure 4), the Bingham yield stress becomes increasingly important and the influence of non-Newtonian nature becomes significant, thereby the relationships between the initial concentration and the advance of current front exhibit a reverse tendency in comparison with that of the dilute counterparts, i.e., the pronounced and sudden arrests appear. This phenomenon is also reflected by the distribution of final deposit densities (Figure 5). For the most dilute case ($c_0 = 0.025$), the maximum deposition density occurs near the release point, and it migrates downstream as the initial concentration increases ($c_0 \le 0.25$). However, as the initial concentration further increases ($c_0 \ge 0.25$), the position of the maximum deposition density migrates upstream, and a step of the final deposition density is resolved and becomes steeper as the initial concentration increases. The implication of the comparison between Case 1 and Case 2 is interesting. The non-Newtonian nature is responsible for the abrupt transitions found in hyperconcentrated turbidity currents. Consequently, existing models for turbidity currents need to be modified to incorporate the non-Newtonian nature in order to be generally applicable. There exist quantitative differences between the numerical (Figures 4 and 5)

and experimental results (Figures 2 and 3). This is ascribable to the approximate description of the non-Newtonian nature. It is appreciated that the use of the Bingham model (Eqs. 9 and 10) in describing the non-Newtonian nature is tentative, and further investigation of the non-Newtonian constitutive relationships of hyperconcentrated turbidity currents is essential.

Physically, the role of non-Newtonian nature in spawning the abrupt transitions in hyperconcentrated turbidity currents may be similar to that for the occurrence of river blockage (stream of essentially vanishing velocity) during the recession phase of hyperconcentrated floods in the Yellow River and its tributaries (China). In both cases, the yield stress hinders the propagation of the flow at high concentrations, and this effect could be overwhelming as the driving force becomes weak (i.e., recession phase of hyperconcentrated flood, and later period of finite-volume lock-release turbidity current).

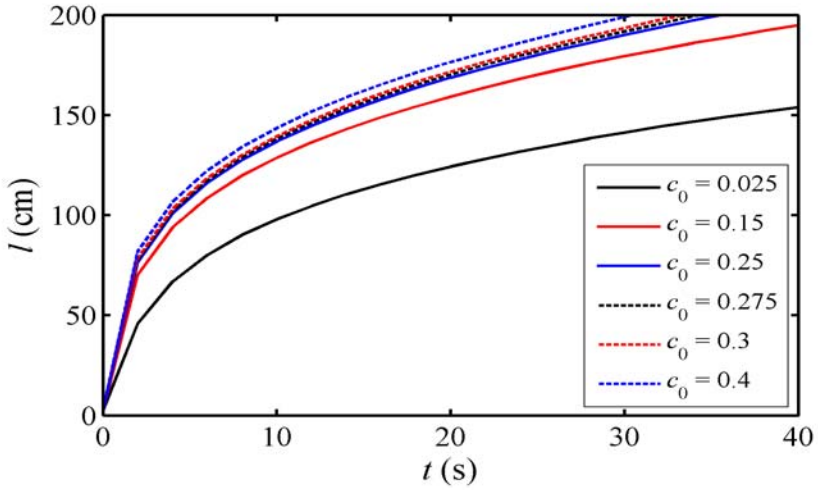

Figure 3. Position of the current front versus t for Case 1 using six different initial sediment concentrations

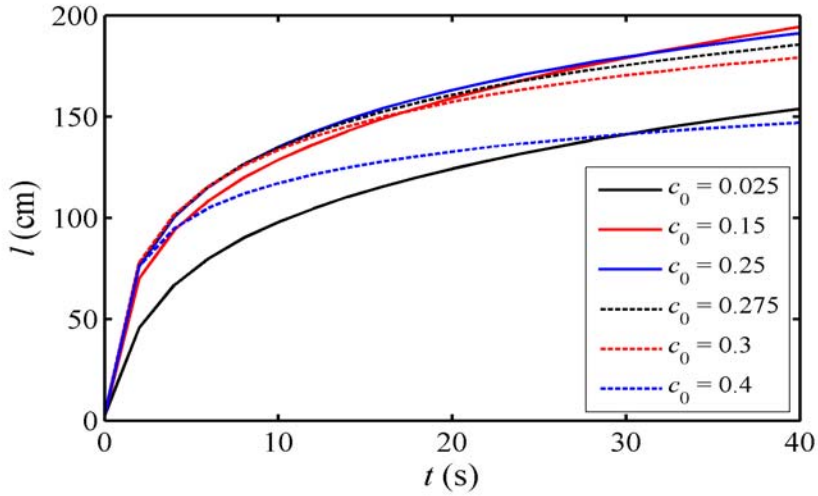

Figure 4. Position of the current front versus t for Case 2 using six different initial sediment concentrations

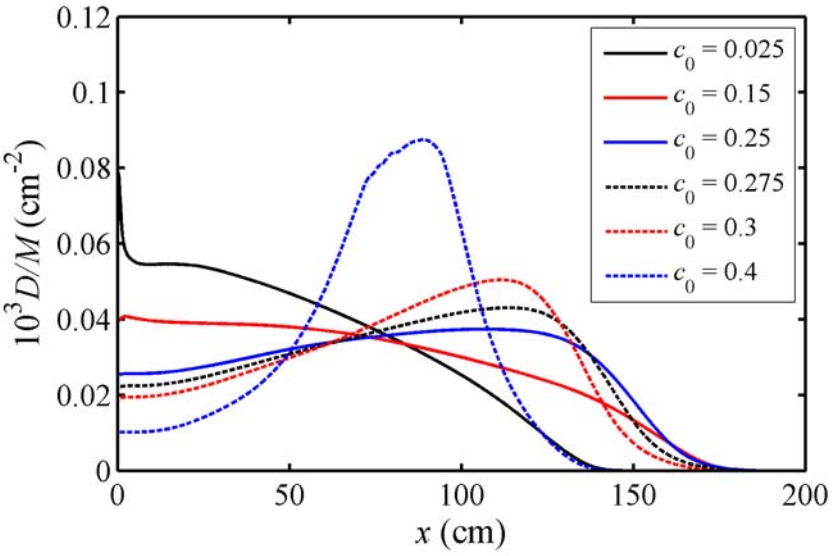

Figure 5. Deposition density $10^3 D / M_0$ versus x for Case 2 using six different initial sediment concentrations

5. CONCLUSION

A layer-averaged fully coupled mathematical model is proposed for hyperconcentrated turbidity currents. Incorporating the non-Newtonian nature of currents at high sediment concentrations, the proposed model qualitatively resolves the abrupt transitions in hyperconcentrated turbidity currents observed by Hallworth and Huppert (1998). This allows us to propose that the non-Newtonian nature may be responsible for the occurrence of abrupt transitions in hyperconcentrated turbidity currents. Also, existing models for turbidity currents need to be modified to incorporate the non-Newtonian nature in order to be generally applicable. It is appreciated that there are inevitable quantitative differences between the numerical simulation and experimental results, which may point to the need for further investigations of physically refined descriptions of non-Newtonian constitutive relationships of hyperconcentrated turbidity currents.

ACKNOWLEDGMENTS

The research reported is funded by the Natural Science Foundation of China (under Grant No. 10672126) and the Doctoral Program Foundation, Ministry of Education, China (under Grant No. 20060486015). The American Institute of Physics is appreciated for the permission for reuse Figure 2 in Hallworth and Huppert (1998).

REFERENCES

Amy, L. A., Hogg, A. J., Peakall, J., and Talling, P. J. (2005), Abrupt transitions in gravity currents, *Journal of Geophysical Research*, AGU, 110(F03001), pp. 1-19.

Bonnecaze, R. T., Hallworth, M. A., Huppert, H. E., and Lister, J. R. (1995), Axisymmetric particle-driven gravity currents, *Journal of Fluid Mechanics*, 294, pp. 93-121.

Bonnecaze, R. T., Huppert, H. E., and Lister, J. R, (1993), Particle-driven gravity currents, *Journal of Fluid Mechanics*, 250, pp. 339-369.

Cesare, G. D., Schleiss, A., and Hermann, F. (2001), Impact of turbidity currents on reservoir sedimentation, *Journal of Hydraulic Engineering*, ASCE, 127(1), pp. 6-16.

Dade, W. B. and Huppert, H. E. (1995), Runout and fine-sediment deposits of axisymmetric gravity currents, *Journal of Geophysical Research*, AGU, 100(C9), pp. 18597-18609.

Gani, M. R. (2004), From turbid to lucid: a straightforward approach to sediment gravity flows and their deposits, *The Sedimentary Record*, SEPM, 2, pp. 4–8.

Hallworth, M. A. and Huppert, H. E. (1998), Abrupt transitions in high-concentration, particle-driven gravity currents, *Physics of Fluid*, 10(5), pp. 1083-1087.

Hu, P. and Cao, Z. (2008), Multiple time scales of turbidity currents and their implications for mathematical modeling, *3rd Sino-American Workshop on Advanced Computational Modeling in Hydroscience & Engineering*, May 13-16, Hawaii, USA.

Huppert, H. E. and Simpson, J. E. (1980), The slumping of gravity currents, *Journal of Fluid Mechanics*, 99, pp. 785-799.

Huppert, H. E. (2006), Gravity currents: a personal perspective, *Journal of Fluid Mechanics*, 554, pp. 299-322.

Inman, D. L., Nordstrom, C. E., and Flick, R. E. (1976), Currents in submarine canyons: an air-sea-land interaction, *Annual Review of Fluid Mechanics*, 8, pp. 275-310.

Kneller, B. and Buckee, C. (2000), The structure and fluid mechanics of turbidity currents: a review of some recent studies and their geological implications, *Sedimentology*, 47, pp. 62-94.

Major, J. J. and Pierson, T. C. (1992), Debris flow rheology: experimental analysis of fine-grained slurries, *Water Resources Research*, 28(3), pp. 841-857.

Middleton, G. V. (1993), Sediment deposition from turbidity currents, *Annual Review of Earth and Planetary Sciences*, 21, pp. 89-114.

Oehy, C. D., and Schleiss, A. J. (2007), Control of turbidity currents in reservoirs by solid and permeable obstacles, *Journal of Hydraulic Engineering*, ASCE, 133(6), pp. 637-648.

Parker, G., Fukushima, Y., and Pantin, H. M. (1986), Self-accelerating turbidity currents, *Journal of Fluid Mechanics*, 171, pp. 145-181.

Pierson, T. C. and Scott, K. M. (1985), Downstream dilution of a lahar–transition from debris flow to hyperconcentrated stream flow, *Water Resources Research*, 21(10), pp. 1511-1524.

Qian, N. and Wan, Z. (1983), *Mechanics of sediment transport*, Beijing: Science Press, China.

Rottman, J. W. and Simpson, J. E. (1983), Gravity currents produced by instantaneous release of heavy fluid in a rectangular channel, *Journal of Fluid Mechanics*, 135, pp. 95-110.

Simpson, J. E. (1997), *Gravity currents in the environment and laboratory*, Cambridge University Press, Cambridge, England.

Toro, E. F. (2001), *Shock-Capturing Methods for Free-Surface Shallow Flows*. Wiley, Chichester, England.

Zhang, R. and Xie, J. (1993), *Sedimentation research in China-systematic selections*, Beijing: China Water and Power Press.

TECHNICAL CONTRIBUTIONS

Flow with Vegetation